

DECORATION OF JOSEPHSON VORTICES BY PANCAKE VORTICES IN $\text{Bi}_2\text{Sr}_2\text{CaCu}_2\text{O}_{8+\delta}$.

V. K. Vlasko-Vlasov¹, A. E. Koshelev¹, U. Welp¹, G. W. Crabtree¹, and K. Kadowaki²

¹*Materials Science Division, Argonne National Laboratory, 9700 South Cass Avenue, Argonne, IL 60439*

²*Institute of Materials Science, The University of Tsukuba, 1-1-1 Tennodai, Tsukuba, 305-8573, Japan*

(November 1, 2018)

Josephson vortices are imaged magneto-optically due to their decoration with pancake vortices in $\text{Bi}_2\text{Sr}_2\text{CaCu}_2\text{O}_{8+\delta}$ single crystals. Peculiarities of interaction between the pancake and Josephson vortices (JV) depending on the values of crossing fields and temperature are studied based on the observations of these decoration patterns. Evidences of the period-doubling in the decoration patterns compared to the JV stack period, migration of JV lines between neighboring stacks, and transitions between different JV configurations are reported. Imaging of the pancake/Josephson vortex decoration patterns over large areas is shown to be a sensitive tool for detecting local variations of the anisotropy and mapping imperfections in layered HTS samples.

I. INTRODUCTION

In strongly anisotropic high- T_c superconductors, such as $\text{Bi}_2\text{Sr}_2\text{CaCu}_2\text{O}_{8+\delta}$ (BSCCO), different magnetic flux components are carried by different types of the magnetic vortices: pancake vortices residing in the cuprate planes are responsible for the perpendicular flux component and Josephson vortices centered between the cuprate planes present the in-plane flux [1–5]. In the first approximation, these two types of vortices are not interacting and form crossing lattices when the external field is not very close to the \mathbf{ab} -plane [6,7]. In this state pancake vortices form a conventional hexagonal lattice which coexists with a stretched hexagonal lattice of Josephson vortices. Due to the large anisotropy γ (~ 500 for BSCCO) the latter arranges into stacks of Josephson lines with large distances between the stacks along the cuprate planes and γ -times smaller inter-vortex separation in the perpendicular direction. It was predicted that the magnetic flux should lock into the ab plane at smaller field angles (to be more precise, if the normal field component is small enough, $H_z < H_{c1}^c$) and form a lattice of tilted vortices when the field is far from the plane [6]. However, the experiment revealed a more complicated picture that can not be explained neglecting the interactions between pancakes and Josephson vortices. An account of these interactions results in a rich phase diagram of various vortex states in inclined fields [8–11] where crossing lattices present the ground state of the superconductor in a wide range of field angles from orientations close to the ab plane to those close to the c axis [9].

Already in the early decoration experiments in BSCCO under inclined fields the formation of vortex rows along the in-plane field has been observed [12,13]. They were initially treated as chains of tilted vortices in accordance with the theory for the moderately anisotropic superconductors [14–16]. In such materials, unlike in the isotropic

case, currents around vortices tilted from the anisotropy directions redistribute so that a magnetic field changes sign on one side of the tilted vortex at some distance from its axis. This field, although weak, attracts neighboring vortices in the tilt plane thus forming chains of inclined vortices. It turned out, however, that in HTS with a weak Josephson coupling between the cuprate layers the scenario is more intriguing. Calculations showed that pancakes and Josephson vortices coexisting in tilted fields attract each other and as a result pancake stacks *decorate* Josephson vortex stacks [9]. A similar explanation of the observed vortex chains in BSCCO, although without supporting calculations, was first suggested in [17]. This decoration effect allows to image otherwise invisible (on the ab plane) Josephson vortices and study their arrangement and changes in layered superconductors (at least in the range of temperatures where the interaction between the Josephson vortices and pancakes is larger than pinning by defects). Recent vortex imaging using scanning Hall probe microscopy gave direct indication for this scenario and for different phases of the interpenetrating pancake and Josephson vortex systems [18]. Also, formation of pancake vortex chains and enhanced mobility of pancakes along the Josephson vortices have been observed recently by the transmission electron microscopy [19]

In the present study we utilize high-resolution magneto-optical imaging [20] to investigate the evolution of the coupled pancake (PV) / Josephson (JV) vortex system in dependence on temperature, applied field, and imperfections in single crystal BSCCO plates. It is revealed that PV/JV coupling is relatively strong and results in a joint motion of both vortex types under the direct action on either of them. We show that in addition to chains of pancake vortices on each JV line at small normal fields there can be superstructures with commensurate decoration patterns (each second JV stack occupied by PVs) as

suggested in [21]. Also, evidence for formation and motion of “dislocations” and “interconnects” in the Josephson lattice in increasing field is presented. A possibility of transitions between two JV lattice configurations resulting in steps on the field dependence of the JV stack period is discussed. We point out that the spacing of Josephson vortex stacks and their mobility is sensitive to the local density of pancakes and the defect structure in the sample. The latter results in spatial variations of the anisotropy and considerable bending of the JV lines.

II. EXPERIMENT AND DISCUSSION

The samples studied here were BSCCO single crystals with as grown flat surfaces and straight edges. T_c of the samples was $\sim 90\text{K}$ as determined from the disappearance of the magneto-optical contrast at the sample edge. The fields parallel and perpendicular to the sample plane were produced by two separate sets of coils positioned outside the optical cryostat, which allowed varying the field components independently. For imaging the normal component of the magnetic induction on the sample surface the magnetic garnet indicators were used as described in a recent review [20]. The indicator film was placed on a flat sample surface and variations of the normal field, B_z , were revealed as local changes of the image intensity in the polarized light microscope. The image intensity can be recalculated into magnetic field values using a calibration procedure. At uncrossed microscope polarizers an increased B_z is revealed either as brighter or darker color of the image depending on the sign of B_z . The field resolution of the technique is of the order of a few tens of milliGauss.

Fig. 1 presents a set of images in the middle of a long BSCCO bar ($3300 \times 850 \times 30 \mu\text{m}^3$) observed in the increasing in-plane field at 85K. The in-plane field direction is indicated by the arrow. The images show dark lines that appear after the application of a small normal field $H_z = 2 \text{ Oe}$ in the presence of the in-plane field. They represent enhanced values of the local magnetic induction and are the manifestation of Josephson vortex stacks decorated by pancake vortices. In small in-plane fields the decorated Josephson vortices are neither regularly spaced nor parallel to the applied field (Fig. 1 a, b). In Fig. 1a there is also evidence for bifurcations of the pattern as discussed in more detail below. Such poor ordering in small in-plane fields is caused by the weak interaction between the distant Josephson vortex stacks. In some regions of the sample only segments of lines were revealed similar to the observations in [18] where 10 times different density of PVs along the same JVs was referred to transitions in PV states on a JV depending on H_z . Buzdin and Baladie [21] showed that PV stacks on a Josephson vortex have a long-range electromagnetic attraction due to their bending by JV currents. This attraction in

balance with a short range repulsion provides an equilibrium distance between PV stacks $a_{eq} \approx 2\lambda_{ab} \ln(1/\epsilon)$, with $\epsilon \approx (\lambda_{ab}/\lambda_J)(B_x/H_o)^{1/4}$ - a parameter characterizing the PV stack bending. Here, λ_{ab} is the in-plane penetration depth, $\lambda_J = \gamma s$ is the JV core size, $H_o = \Phi_o/\gamma s^2$, Φ_o - the flux quantum, and s is the cuprate layer spacing. Above relation is valid if $a_{eq} < \lambda_J$. Note, that the equilibrium separation between PVs on a JV stack is controlled only by the in-plane field B_x and this dependence is extremely weak. In small H_z the available amount of pancakes is not sufficient to fill all JV stacks with the optimal PV density. In this case pancakes can gather (due to the long range character of attraction) into dense clusters where PVs are separated by a_{eq} leaving the other parts of JV empty. This could explain our observations of segments of lines in the decoration patterns if to admit that the access of PVs is restricted in the areas where fragmented JV lines are revealed. In support of such situation we will show below that the inhomogeneous penetration of the normal field is a common feature revealed in all studied BSCCO crystals.

With increasing H_x the pattern regularity improves. The PV lines orient along the field, become more periodic, and the period decreases as H_x increases (Fig. 1c). At larger H_x the MO contrast drops but the regularity of the JV stacks is well revealed at differences of images taken at $H_z = 0$ and 2 Oe in the same H_x (Fig. 1d). Such a procedure reduces the optical noise and allows to observe much weaker features.

The improvement of the PV line pattern with H_x can be explained by increasing the number of PV/JV intersections and the equilibrium density of PV stacks ($\sim 1/a_{eq}$). As it was calculated in [9] the intersection of a Josephson vortex and a pancake line produces a negative (attractive) contribution to the energy of both vortices due to the shift of PVs by the Lorentz force of JV currents. The main contribution to the crossing energy E_{\times} comes from pancakes nearest to the JV and is given by

$$E_{\times} = -2.1(\Phi_o^2/4\pi^2\gamma^2s) \ln(3.5\lambda_J/\lambda_{ab})$$

Clearly the total gain of energy ΔE_{cr} will increase with the number of intersections $N \sim 1/d$ where $d = [2\Phi_o/\gamma H_x]^{1/2}$ is the distance between JVs in a stack along the c -axis. Thus the energy gain of the PV line crossing the JV stack compared to the energy of the noncrossing PV line $E_{pv} = (\Phi_o/4\pi\lambda_{ab})^2 \ln(\lambda_{ab}/\xi_{ab})$ will be

$$\Delta E_{cr}/E_{pv} = -\frac{8.4(\lambda_{ab}/\lambda_J)^2}{\ln(\lambda_{ab}/\xi_{ab}) \ln(3.5\lambda_J/\lambda_{ab})} (s/d)$$

(see also [11]). Taking for BSCCO $\lambda_{ab}(T=0) = 2000\text{\AA}$, $\xi_{ab}(0) = 30\text{\AA}$, $s = 15\text{\AA}$, and $\gamma = 500$, one gets $|\Delta E_{cr}|/E_{pv} = 0.055(s/d)$ at low T.

The energy of the electromagnetic coupling between PV lines at the equilibrium distance a_{eq} on a JV stack [21] normalized to the energy of noninteracting lines gives

$$\Delta E \approx \frac{-2(s/d)[1/\ln(\lambda_{ab}/\xi_{ab})]}{\left[(\lambda_J/\lambda_{ab}) \ln(\lambda_J/\lambda_{ab}) \ln[\sqrt{s/d}(\lambda_J/2\lambda_{ab}) \ln(\lambda_J/\lambda_{ab})]\right]^2}$$

For comparison with ΔE_{cr} (at low T) we write this ratio in a similar form $|\Delta E_{em}|/E_{pv} \sim 0.0017(s/d)$ at $H_x=1$ Oe and $\sim 0.0039(s/d)$ at $H_x=100$ Oe (the effect of (s/d) under the ln is not large). This shows that the major gain of energy due to the decoration of JV stacks by pancakes is provided by ΔE_{cr} and ΔE_{em} gives only minor contribution. Formally it is clear from the ratio

$$\Delta E_{em}/\Delta E_{cr} \approx \frac{4(\lambda_{ab}/a_{eq})^2}{\ln(\lambda_J/\lambda_{ab})}$$

As follows from the above formulas, the *relative contribution* of interactions in the PV line energy should strongly increase near T_c due to the temperature dependence of λ_{ab} . Both E_x and E_{em} are only weakly (logarithmically) dependent on λ_{ab} and thus on T. However, the reference energy of a noninteracting PV line decreases near T_c as $\sim \lambda_{ab}^2$, which strongly increases the relative effects of E_x and E_{em} . Actually, these effects should logarithmically diverge at $T_d=86.5$ K, where $\lambda_{ab}(T) = \lambda_{ab}(0)/[1 - (T/T_c)^2]^{1/2} \rightarrow \lambda_J$ (here $T_c=90$ K). However, the theory is developed for $\lambda_{ab} < \lambda_J$ and it becomes inapplicable near T_d . We imaged decorated Josephson stacks in the temperature range from 60 K to 88 K. The patterns were poor at lower T and at $T>87$ K, and the cleanest patterns were observed around 85 K. This is in accordance with the increasing role of E_x and E_{em} at larger temperatures and successive instability of the crossing lattice configuration when $\lambda_{ab} \geq \lambda_J$. Note that the MO contrast of the pattern should decrease with temperature due to the decrease of equilibrium decorating PV density $1/a_{eq} \sim 1/\lambda_{ab}$. Another factor that could facilitate in the formation of optimum pattern at ~ 85 K is the balance between pinning restricting the mobility of pancakes at lower temperatures and thermal disordering washing out the vortex lattices at higher temperature. We note that in HTS at high T effects of correlated pinning (on extended defects such as twins or columnar defects) become more effective. This would extend the limits of stability of the PV/JV decoration patterns. These patterns (although with a weak contrast and only at larger fields) have been revealed even at $T=88$ K (see Fig.2c,d).

At a given field H_x the only parameter controlling the period of the stacks of Josephson vortices is the anisotropy γ . This was used in [18] for extracting γ from the decoration patterns observed in relatively small area ($\sim 25 \times 25 \mu m$). Our observations in larger regions ($\sim 500 \times 500 \mu m^2$) revealed that the period can vary across the sample even in high in-plane fields and well developed patterns as is shown in Fig. 2. This effect can have several reasons. First, there can be local changes of the anisotropy associated with composi-

tional and structural variations in the sample. It is typically observed in BSCCO that irregularities of the crystal structure show up at relatively high temperatures due to "balloons" of increased B_z formed at them [20,21]. We observed that at small normal fields B_z inhomogeneities in our samples serve as seeding areas from which PVs spread along the JV stacks. Similar channeling of PVs along JVs was reported in [18]. In the vicinity of the increased B_z spots the decoration pattern showed smaller periods at all fields. This can be associated with compositional variations of the anisotropy (e.g. increased oxygen concentration should reduce γ [24] and thus the period). However, in some areas the difference in period compared to the neighboring regions was found to disappear at increasing field. This could be due to a possibility of two different JV configurations as shown in Fig.3, which have different relations for the stack periods (D) and distances between JVs in the stack (d): $D_1 = (\sqrt{3}\gamma\Phi_o/2H_x)^{1/2}$, $d_1 = (2\Phi_o/\sqrt{3}\gamma H_x)^{1/2}$, and $D_2 = (\gamma\Phi_o/2\sqrt{3}H_x)^{1/2}$, $d_2 = (2\sqrt{3}\Phi_o/\gamma H_x)^{1/2}$, respectively. Within the anisotropic London model such vortex configurations have the same energy when the field is along the ab plane [25]. This degeneracy, however, is lifted and the first configuration becomes preferential when the perpendicular field is applied [25]. In the case of the layered systems in the crossing fields the difference in the energy of the configurations will be due to different number of PV/JV intersections. For one PV line intersecting a JV stack this difference will be $\Delta E_{cr} \sim E_x \cdot (1/d_1 - 1/d_2)$ which also gives preference to the first configuration ($d_1 < d_2$). However, this preference is very small. Assuming the equilibrium distances between PV lines on JV stacks the total number of intersections per unit volume in each configuration will be $N_{cr} \sim 1/d \cdot 1/D \cdot 1/a_{eq}$. In this case the difference in the gain due to the crossing energy between them totally disappears ($d_1 D_1 = d_2 D_2$). The average value of B_z will be slightly different for the two configurations. However, due to the inhomogeneities in the samples tuning of the local $\langle B_z \rangle$ can be easily realized. Therefore one can expect that these configurations could coexist in the samples and transform from one to another causing changes of the decoration pattern period. In the increasing in-plane field both distances between the stacks, D , and spacing between JVs along the c -axis, d , should decrease. For tuning D Josephson vortices easily slide along the cuprate planes. However, to tune d they have to traverse the planes which requires overcoming a considerable energetic barrier and makes this process much slower. It can be probably done only by formation of double kinks or kinks coming from the edges and their recession along the planes as in the case of dislocations moving from one crystal plane to another [26]. It is reasonable to suggest that the system is not in the equilibrium state at all fields but transforms through a set of metastable states admitting a mixture of the above two possible JV config-

urations and transitions between them. A whole series of other JV configurations (with different D/d ratios) transforming from one to another in small H_x were predicted for the situation when JV vortices can not move along the c axis at all [27]. Stepwise transitions between different JV configurations in higher fields were discussed recently in [28]. A possible confirmation of the above scenario is the $D^{-2}(H_x)$ dependence shown in Fig. 4. Minimum, maximum and average periods of the decoration pattern plotted on this graph were measured over a large area ($500 \times 500 \mu m^2$) in the middle of the crystal. The data definitely show a number of steps which can be associated with impeding of the JV system tuning and possibly transitions between different JV lattice configurations. At the same time, the overall changes of the decoration pattern period is well described by a linear dependence D^{-2} vs. H_x and give reasonable values of the anisotropy from 570 to 700.

Another kind of variation of the pattern period was observed at moderate in-plane fields and at higher temperatures when areas showing the same anisotropy in larger H_x unexpectedly reveal periods differing by a factor of two. Fig. 5a, b show such an area where the distance between decorated JV stacks increases with increasing field in contradiction to theory. However, the pattern in nearby areas (Fig. 5c) where the period decreases with increasing H_x in a regular way displays half of the period seen in the anomalous areas. This indicates that the large period reveals only each second JV stack. The possibility of the formation of PV chains at integer numbers of JV periods was considered recently by Buzdin and Baladie [21]. They show that the equilibrium density of PV lines decorating JV stack ($1/a_{eq}$) is practically field independent (it is a very weak function of H_x only). So at low B_z there are not enough pancakes to decorate all the JV stacks with this density and a superstructure of decorated and non-decorated stacks develops. With increasing B_z the density of chains increases and finally all JV stacks become occupied with PV. In large B_z pancakes start spreading into the volume between the JVs. Obviously, in our samples inhomogeneities of the PV concentration caused by crystal imperfections determine the domains where local conditions for superstructures are provided. We already exploited the argument of equilibrium PV spacing to explain the observation of segmented decoration lines. To explain the commensurate periodic patterns one has to account also for the long range repulsion between pancakes on different stacks. This could be due to the Pearl's interaction [29] through the stray fields of pancakes at the sample surface. Although these interactions are long range but they are weak and their effect should be noticeable only in favorable conditions. Probably this is the reason why the superstructure was observed only at high temperatures and only in some parts of the sample.

The picture of the field transformations of the JV lat-

tice discussed above suggests that there should be defects in the JV stack arrangement. In particular, we observed interconnects and "dislocations" in the regular decoration line arrays as illustrated in Fig.6. It is known that JV lines do not split or terminate inside a superconductor. Therefore, the decoration pattern reveals the migration of Josephson vortices between different stacks. A corresponding scheme of JV kinks visualized due to PV stacks of different length is shown at the bottom of Fig.6. The kinks can form at different depth from the surface and still they will be decorated by PV stacks if this depth is not too large. On the left scheme two possible variants of JV travelling between the stack is shown but only one of them corresponds to the pattern in Fig.6a. Note, that in either case the kinks in neighboring stacks are located between different cuprate planes. This means that defects in the decoration pattern reveal also defects in ordering of Josephson vortices in the stacks along the c -axis. Comparison of Fig.6b and c shows that JV kinks shift along the direction of H_x at changing field. As a result the defects are removed from the decoration pattern at large in-plane fields.

Difference images presented in Figs.6b and c illustrate one more important feature of the JV behavior. The first picture corresponds to the increase of H_x by 2 Oe and the second one to the increase of H_z by the same 2 Oe. Old positions of JV stacks are revealed as brighter lines and new positions are seen as dark lines (the direction of motion is shown by arrow on the top). It is easy to see that at $T \sim 85K$ and $H_x \sim 25$ Oe the change of H_z shifts JVs by nearly the same distance as a similar change of H_x . This is a direct evidence of the strong coupling between the two systems of vortices. It also reveals a possibility to move Josephson vortices either directly acting on them by the in-plane field or by shifting coupled to them pancake vortices by the normal field.

Another illustration of strong interactions between the two components of magnetic flux in BSCCO is the effect of B_z inhomogeneities on bending JV stacks. Fig.7a-b presents two successive images taken at increasing H_z from 5 to 8 Oe in a sample field cooled to 83K in $H_x = 18.5$ Oe. Dark spots on the pictures correspond to increased B_z at structural imperfections of the crystal as discussed before. Dark lines are JV stacks decorated by PVs. Upon ramping H_z up the increased B_z region in the left bottom corner expands and shifts decorated JV stacks considerably bending them. Fig.7c shows that Josephson vortices can also strongly bend during their evolution in the in-plane field when they cross the B_z inhomogeneities. This picture presents the difference of images at $H_x = 12$ and 14 Oe. A rounded area in the middle of the picture is the spot of increased B_z . It is not dark because at original images B_z in this spot did not change. Here JV lines are not revealed because they did not move at changing H_x being pinned by the large density of PVs. The break of angle of the Josephson vortices in this spot is well seen.

In general, the JV stacks in the crossing fields are clearly seen on the background of the inhomogeneous B_z distribution as shown on a panoramic MO picture near the corner of a BSCCO crystal in Fig.8. They form an intricate pattern of curved lines (it straightens up at larger H_x) which can be a sensitive tool for studying crystal imperfections and spatial anisotropy variations.

III. CONCLUSIONS

We studied magneto-optically the behavior of the decoration of Josephson vortices by pancake vortices in the single crystals of BSCCO. The decoration pattern turns out to be robust in a wide range of temperatures and fields. Simultaneous imaging of a large area accessible by the MO technique allows to observe interactions of the Josephson vortices with sample imperfections and through the measurements of JV stack periods to map spatial variations of the anisotropy of the sample. The experiment reveals a strong coupling between pancake and Josephson vortices which shows up through the motion of both flux components under the direct action on one of them and pinning and bending of JV lines at the inhomogeneities of the pancake density (B_z). At larger temperatures the quality of the decoration pattern improves which can be referred to (a) the relative increase of the energy of PV/JV interactions compared to the energy of noninteracting pancakes and (b) the increase of the role of correlated pinning of pancakes on the nearly 2D JV stacks. Possible evidences of the coexistence of two different JV lattice configurations are observed. Also intrinsic defects of the JV lattice like “interconnects” and “dislocations” are revealed that are associated with wandering of the Josephson vortices between neighboring stacks. At small fields commensurate patterns with each second JV stack decorated by pancakes are found in accordance with recent theoretical predictions.

ACKNOWLEDGMENTS

The authors thank A. I. Buzdin and S. Bending for stimulating discussions and presentation of his results prior to publication. The work was supported by the U.S.DOE, BES-Materials Sciences, under Contract #W-31-109-ENG-38.

- [4] P. H. Kes, J. Aarts, V. M. Vinokur, and C. J. van der Beek, Phys. Rev. Lett. **64**, 1063 (1990).
- [5] S. Theodorakis, Phys. Rev. B **42**, 10172 (1990).
- [6] L. N. Bulaevskii, M. Ledvij, and V. G. Kogan, Phys. Rev. B **48**, 366 (1992).
- [7] M. Bencrouda and M. Ledvij, Phys. Rev. B **51**, 6123 (1995).
- [8] L. N. Bulaevskii, M. Maley, H. Safar, and D. Dominguez, Phys. Rev. B **53**, 6634 (1996).
- [9] A. E. Koshelev, Phys. Rev. Lett. **83**, 187 (1999).
- [10] S. E. Savel'ev, J. Mirkovich, and K. Kadowaki, Phys. Rev. B **64**, 094521 (2001).
- [11] M. J. W. Dodgson, cond-mat/0201197 (2002).
- [12] C. A. Bolle, P. L. Gammel, D. G. Grier, C. A. Murray, and D. J. Bishop, Phys. Rev. Lett. **66**, 112 (1991).
- [13] I. V. Grigorieva, J. W. Steeds, G. Balakrishnan, and D. M. Paul, Phys. Rev. B **51**, 3765 (1995).
- [14] A. I. Buzdin and A. Yu. Simonov, JETP Lett. **51**, 191 (1990).
- [15] A. M. Grishin, A. Yu. Martynovich, and S. V. Yampolskii, Sov. Phys. JETP **70**, 1089 (1990).
- [16] V. G. Kogan, N. Nakagawa, and S. L. Thiemann, Phys. Rev. B **42**, 2631 (1990).
- [17] D. Huse, Phys. Rev. B **46**, 8621 (1992).
- [18] A. Grigorenko, S. Bending, T. Tamegai, S. Ooi, and M. Henini, Nature **414**, 728 (2001).
- [19] T. Matsuda, O. Kamimura, H. Kasai, K. Harada, T. Yoshida, T. Akashi, A. Tonomura, Y. Nakayama, J. Shimoyama, K. Kishio, T. Hanaguri, and K. Kitazawa, Science, **294**, 2136(2001)
- [20] V. K. Vlasko-Vlasov, U. Welp, G. W. Crabtree, and V. I. Nikitenko in *Physics and Materials Science of vortex states, flux pinning and dynamics* (eds. R. Kossowsky et al., NATO Science Series E) **356**, 205-237 (Kluwer Academic Publishers, Dordrecht, Boston, London, 1999).
- [21] A. Buzdin and I. Baladie, cond-mat/0110339 (2001).
- [22] A. Soibel, E. Zeldov, M. Rapoport, Yu. Myasoedov, T. Tamegai, Sh. Ooi, M. Konczykowski, and V. B. Geshkenbein, Nature **406**, 282 (2000).
- [23] G. Yang, J. S. Abell, and C. E. Gough, Physica C **341-348**, 1091 (2000).
- [24] Y. Kotaka, T. Kimura, H. Ikuta, J. Shimoyama, K. Kitazawa, K. Yamafuji, K. Kishio, and D. Pooke, Physica C **235-240**, 1529 (1994).
- [25] L. J. Campbell, M. M. Doria, and V. G. Kogan, Phys. Rev. B **38**, 2439 (1988).
- [26] J. P. Hirth and J. Lothe, Theory of Dislocations, Wiley, New York (1982).
- [27] L. S. Levitov, Phys. Rev. Lett. **66**, 224 (1991).
- [28] J. Mirkovic, S. E. Savel'ev, E. Sugahara, and K. Kadowaki, Phys. Rev. Lett. **86**, 886 (2001).
- [29] J. Pearl, Appl. Phys. Lett. **5**, 65 (1964).

[1] A. Buzdin and D. Feinberg, J. Phys. **51**, 1971 (1990).

[2] J. R. Clem, Phys. Rev. B **43**, 7837 (1991).

[3] S. N. Artemenko and A. N. Kruglov, Phys. Lett. **83** 485 (1990).

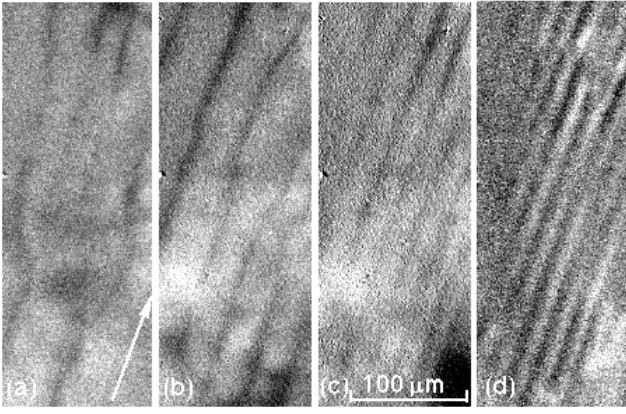


FIG. 1. Lines of increased B_z (dark) at stacks of Josephson vortices at changing in-plane field. $H_z=2$ Oe, H_x for (a) to (d): 3, 12, 24, and 42 Oe. A ratio of images ($\uparrow 2, 42$)/(0,42) in (d) reveals better the positions of JV stacks. $T=85$ K.

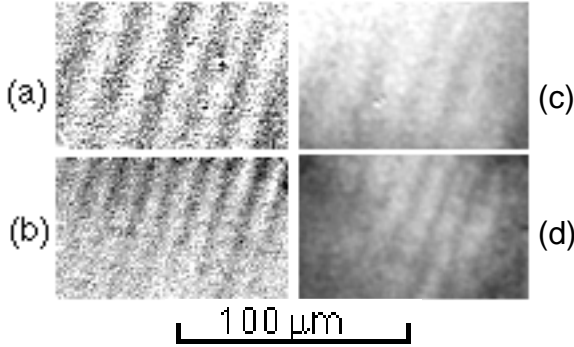


FIG. 2. Different periods of MO patterns in different spots distant by $600 \mu\text{m}$ ((a) and (b) at 84K, (c) and (d) at 88K) in a BSCCO crystal. Ratios of images $(H_z, H_x) = (\uparrow 2, 40)/(0, 40)$ Oe are shown.

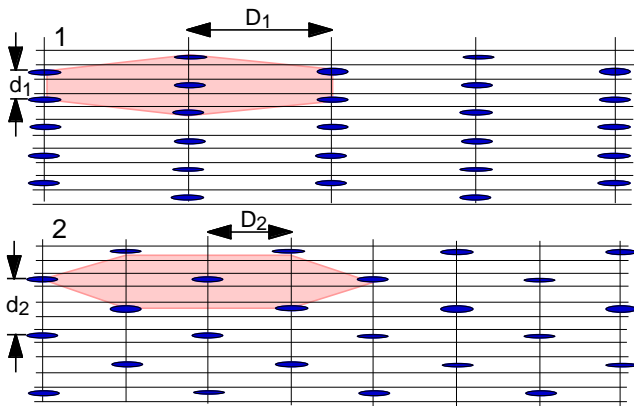


FIG. 3. Schematic for two different Josephson vortex configurations in a layered superconductor (for $\gamma \sim 5$) which are degenerate in energy at $H \parallel$ cuprate planes. For BSCCO the picture should be stretched along X and compressed along Y ~ 10 times.

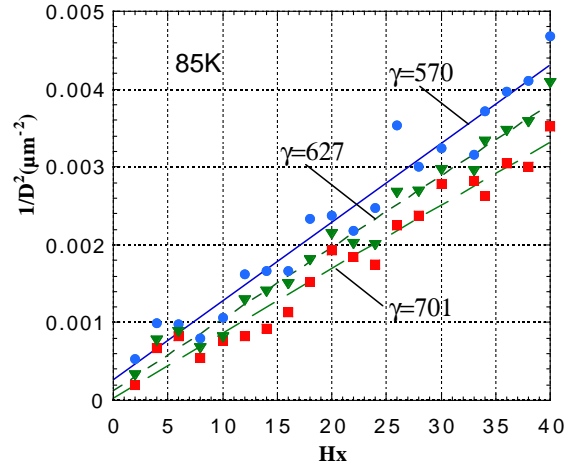


FIG. 4. Field dependence of the decoration pattern period. Linear fit for $1/D^2 - H_x$ gives estimates for the anisotropy for min, max, and average periods as shown on the graph.

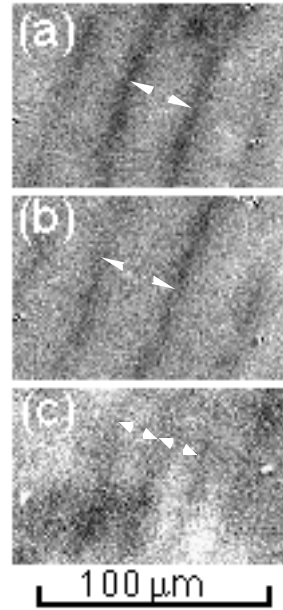


FIG. 5. Increase of the decoration pattern period (marked by arrows) at increasing in-plane field from 15 Oe in (a) to 21 Oe in (b). (c) Twice smaller period revealed in the neighboring area at 21 Oe. $T=83$ K, $H_z=2$ Oe.

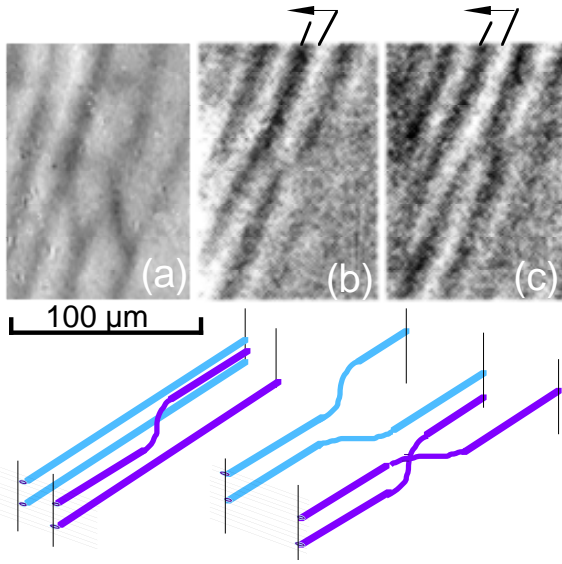


FIG. 6. Interconnects and dislocation like structures in the JV decoration patterns. (a) Difference of MO images at $(H_z, H_x) = (2, 18.5)$ and $(0, 18.5)$ Oe, $T = 83$ K. (b) Difference of images at $(H_z, H_x) = (0, 26)$ and $(0, 24)$ Oe, JVs carry PVs captured after previous application of $B_z = 2$ Oe, $T = 85$ K. (c) Difference of images at $(H_z, H_x) = (2, 26)$ and $(0, 26)$ Oe, $T = 85$ K. Schematics of kinks at Josephson vortices rerouting them between neighboring stacks are shown in the bottom. Left scheme corresponds to (a) and right to (b-c). Vertical lines on the schematics mark positions of JV stacks. Horizontal lines show cuprate planes.

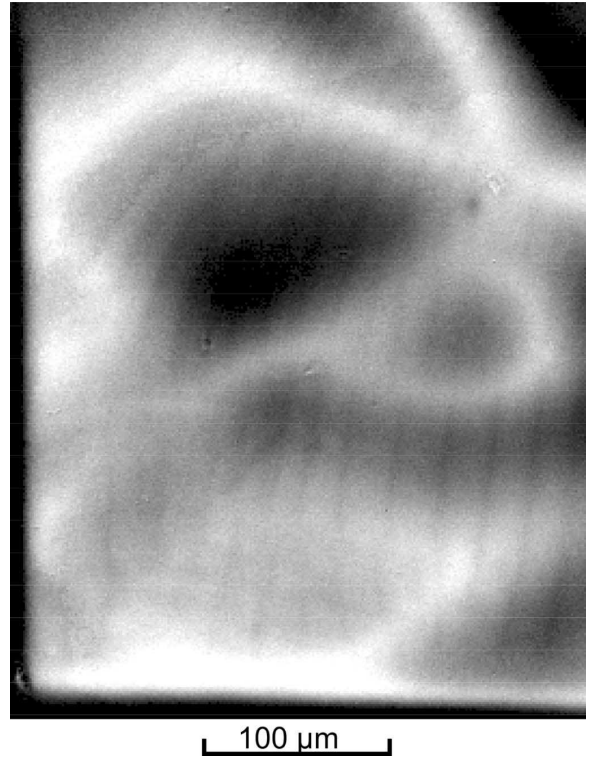


FIG. 8. Josephson vortex stacks (dark lines in vertical direction) visualized at $H_z = 22$ Oe $H_x = 20$ Oe, $T = 83$ K. Brightness of the image corresponds to the local B_z in the sample. Left and bottom sides of the picture are crystal edges.

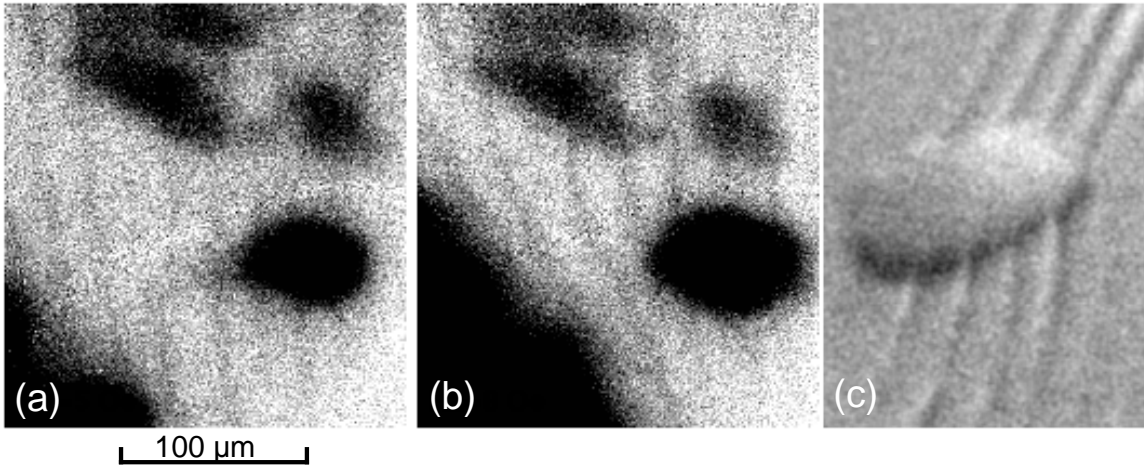


FIG. 7. (a-b) Bending of Josephson vortices (dark lines in y-direction) at spots of increased B_z (dark). (a) $H_z = 5$ Oe, (b) $H_z = 8$, $T = 83$ K. The sample is cooled in $H_x = 18.5$ Oe. (c) The difference of MO images taken at changing H_x from 12 to 14 Oe near the spot of increased B_z (rounded area in the center). $H_z = 10$ Oe, $T = 80$ K. JVs have shifted from bright to dark positions.